Materials Research, Vol. 7, No. 1 , 81-88, 2004.

Stress and Adhesion of Chromia-Rich Scales on Ferritic Stainless Steels in Relation with Spallation

A. Galerie[a], F. Toscan[a], M. Dupeux[a], J. Mougin[b], G. Lucazeau[c], C. Valot[d], A.-M. Huntz[e], L. Antoni[f]*

[a]*Laboratoire de Thermodynamique et de Physicochimie Métallurgiques*
Unité Mixte de Recherches CNRS/UJF/INPG, 5614,
BP 75 F-38402 Saint Martin d'Hères Cedex, France
[b]*Dept. FMC, ASCOMETAL-CREAS,Lucchini Group,*
BP 70045, 57301 Hagondange Cedex, France
[c]*Laboratoire d'Electrochimie et de Physicochimie des Matériaux et des Interfaces*
Unité Mixte de Recherches CNRS/UJF/INPG, 5631
BP 75 F-38402 Saint Martin d'Hères Cedex, France
[d]*Laboratoire de Recherches sur la Réactivité des Solides*
Unité mixte de Recherches, 5613, Faculté des Sciences Mirande, 9 Allée Alain Savary
BP 47870, F-21078 Dijon Cedex, France
[e]*Laboratoire d'Etudes des Matériaux Hors Equilibre*
Unité Mixte de Recherches, 8647, Université de Paris-Sud,
Centre d'Orsay, F-91405 Orsay, France
[f]*Commission à I'Energie Atomique, Centre de Grenoble – DTEN / SCSE / LHPAC*
17 rue des Martyrs, 38054 Grenoble Cedex 9, France

Received: September 2, 2002; Revised: September 4, 2002

The relation between chromia scale spallation during oxidation or cooling down of ferritic stainless steels is generally discussed in terms of mechanical stresses induced by volume changes or differential thermal expansion. In the present paper, growth and thermal stress measurements in scales grown on different ferritic steel grades have shown that the main stress accumulation occurs during isothermal scale growth and that thermal stresses are of minor importance. However, when spallation occurs, it is always during cooling down. Steel-oxide interface undulation seems to play a major role at this stage, thus relating spallation to the metal mechanical properties, thickness and surface preparation. A major influence on spallation of the minor stabilizing elements of the steels was observed which could not be related to any difference in stress state. Therefore, an original inverted blister test was developed to derive quantitative values of the metal-oxide adhesion energy. These values clearly confirmed that this parameter was influenced by scale thickness and by minor additions, titanium greatly increasing adhesion whereas niobium decreased it.

Keywords: *chromia scales, oxide stress, oxide adhesion, ferritic stainless steels*

1. Introduction

Ferritic stainless steels can be used in high temperature situations where mechanical solicitations are not too severe. They present the advantage over the austenitic grades to faster passivate and reheal due to the high chromium diffusivity in the non compact bcc structure. Moreover, they suffer less from scale spallation at cooling, resulting from their lower thermal expansion coefficient (TEC). In addition, the absence of nickel makes them of more regular price, what is economically interesting. That is the reason why their use in exhaust systems (tubes, pipes, manifolds, flexible

*e-mail: alain.galerie@ltpcm.inpg.fr
Presented at the International Symposium on High Temperature Corrosion in Energy Related Systems, Angra dos Reis - RJ, September 2002.

couplings) allows to reduce weight compared to the use of thick cast iron or carbon steel parts.

However, their performances may be increased, for example by retarding, reducing or suppressing scale spallation under cyclic conditions. As spallation is thought to be the result of growth and/or thermal stress accumulation leading to oxide-steel interface decohesion, it is of importance to separate stress and adhesion effects. This paper presents quantitative measurements of growth and thermal stresses and of oxide-substrate adhesion energy on several ferritic stainless steel grades and discusses their relation to scale spallation.

2. Experimental

2.1. Materials

The materials under study were four ferritic stainless steel grades with 18% chromium, with or without the bcc stabilisers Ti and Nb. Their chemical compositions are given in Table 1. They were used in form of sheets, with 3 different thicknesses : 1.50, 0.60 and 0.15 mm. The two thickest sheets were polished under water before oxidation, generally up to 1 200 SiC grit. The 0.15 mm thick foils were used in their industrial surface finish, only ultrasonically degreased and rinsed.

2.2. Oxidation procedures

Isothermal and cyclic oxidation conditions were used in the present study. Isothermal tests were conducted at 900 °C in a horizontal furnace under 150 mbar O_2 or H_2O partial pressure and 1 bar total pressure, with argon as a carrier gas. Cyclic tests were performed in laboratory air by automatic immersion-emersion of samples in a vertical furnace set at 850 °C, with the following cycle parameters:

- heating time at immersion (to reach 840 °C): 13 min,
- dwell time at 850 °C: 20 min,
- forced air cooling down to 100 °C at emersion: < 1 min, total cooling time: 5 min.

8 to 24 samples could be oxidised simultaneously in such a device[1]. After oxidation, the specimens were weighed and image analysis was used to assess the spalled fraction of the surface area.

For *in situ* Raman spectroscopy experiments under both oxygen or water vapour, 750 °C was the maximum temperature which could be achieved in the laboratory-made furnace used[2]. Oxygen and water vapour pressures used were 150 mbar and 26 mbar respectively, with argon completing to 1 bar.

2.3. Stress determination

Stresses in chromia scales were mainly determined by Raman spectroscopy, using the A_{1g} line of Cr_2O_3 appearing at ≅ 549 cm^{-1} for unstressed scales on stainless steels and linearly shifting with hydrostatic pressure to higher wavenumbers according to[2,3,4]:

$$\sigma\,(\text{GPa}) = 0.307 \pm 0.005\ \Delta nu\ (\text{cm}^{-1}) \qquad (1)$$

In situ measurements were performed between room temperature and 750 °C, either during isothermal O_2 or H_2O exposure or during temperature changes. Residual stress measurements were also performed at room temperature after isothermal oxidation at 900 °C and cooling down. Comparative measurements using room temperature X-Ray diffraction and deflection during temperature changes of monofacially oxidised samples were used as Raman calibrations[5,6], showing that Eq. 1 should be directly used for the present measurements without any biaxial correction, although such a correction is generally suggested in the literature[7,8].

2.4. Adhesion measurements

For quantitatively measuring the scale-metal adhesion energy, a modified inverted blister test was used [9,10,11]. It allowed to grow a circular interfacial crack by pushing pressurised water through a hole in the oxide, forcing the metal to form a blister. From the pressure (P) – blister height (h) relation, the adhesion energy G_i was derived, according to:

$$G_i = C.P.h \qquad (2)$$

with C a dimensionless constant depending on the test geometry ; its value is 0.62 in the present work.

3. Results

3.1. Factors influencing spallation

When oxidised isothermally in oxygen, stainless steel samples never spall during the temperature plateau. At cool-

Table 1. Chemical composition of the ferritic grades (weight %).

Grade	AISI	Fe	Cr	Ti	Nb	Mn	Si	C	S
Fe-18Cr	430	Bal.	18.1	/	/	0.11	0.51	0.01	0.0008
Fe-18Cr-Ti	439	Bal.	17.7	0.45	/	0.42	0.62	0.04	0.0007
Fe-18Cr-Nb	/	Bal.	17.5	/	0.44	0.30	0.64	0.02	0.0012
Fe-18Cr-TiNb	441	Bal.	17.6	0.14	0.47	0.28	0.57	0.02	0.0008

ing, they exhibit different amounts of spallation, depending on the nature of their stabilising addition element (Fig. 1). Compared to the reference grade Fe-18Cr that began to spall for 1.5 µm thick oxide scales, the Fe-18Cr-Ti and Fe-18Cr-TiNb grades did not spall in the thickness range studied, whereas the Fe-18Cr-Nb grade presented extensive scale loss. The respective good and bad effects of Ti and Nb are here clearly demonstrated. A large influence of substrate thickness was also observed and is depicted in Fig. 2 where it is shown that the thicker the substrate, the more extensive is spallation. Changing the atmosphere from oxygen to pure water vapour changed drastically the behaviour as, for the same oxide thickness isothermally generated on the same grades, no spallation was observed in H_2O.

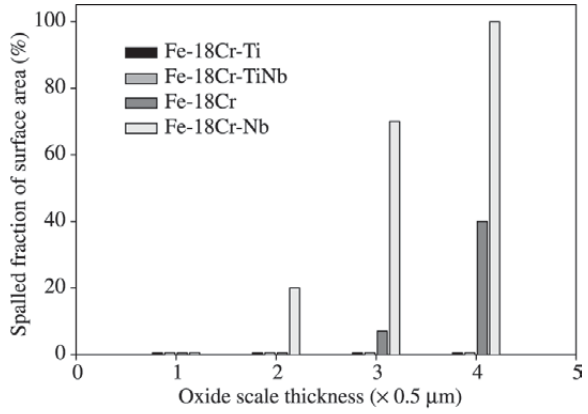

Figure 1. Oxide spallation average data at cooling after isothermal oxidation in oxygen as a function of scale thickness for the ferritic grades under study (substrate thickness: 0.15 mm).

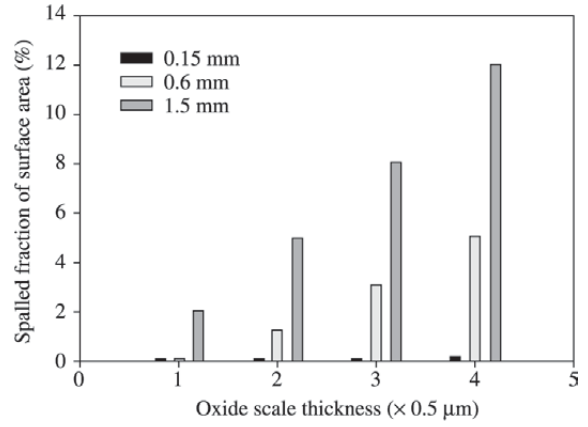

Figure 2. Oxide spallation average data at cooling after isothermal oxidation in oxygen as a function of substrate thickness for the bi-stabilised Fe-18Cr-TiNb grade.

Spallation in cyclic oxidation experiments was not evidenced from the weight gain vs. time curves, which presented continuous near-parabolic weight increase. Surface observations after 150 and 300 cycles showed very few bare metal areas as shown by Table 2. It should be noted however that such observations do not take into account earlier spallation followed by scale reformation. Anyway, even with low spallation, the tendency in thermal cycling was exactly the same as in isothermal conditions, with no spallation for the two Ti-containing grades, a little for the reference grade Fe-18Cr and the maximum for the Fe-18Cr-Nb.

For better comparison with Fig. 1, the respective thickness of the oxide scales have been included in Table 2. Due to its high growth rate, the very adherent scale on Fe-18Cr-Ti is the thickest of all grades.

3.2.Stress results

Oxide growth stresses in oxygen determined at 750 °C on the reference grade Fe-18Cr and on the bi-stabilised Fe-18Cr-TiNb grade were always compressive (Fig. 3). They showed a very rapid increase during the initial oxide growth up to a thickness of ~ 0.2 mm. For this thickness, high values were achieved, in the range – 2 to – 3 GPa. Initially they were a little higher for the reference grade, but slowly decreased with time, whereas the Fe-18Cr-TiNb grade seemed to keep a near-constant value up to an oxide thickness of ~ 0.5 µm.

In water vapour, for oxide scales grown at the same temperature under 26 mbar H_2O pressure, the growth stresses determined on the Fe-18Cr reference grade were slightly lower than when grown in oxygen, rapidly attaining a – 1.8 GPa plateau.

Thermal stresses were determined *in situ* by observing the Cr_2O_3 Raman shift at cooling from 750 °C to room temperature (circular points in Fig. 4). Three important conclusions were drawn from these measurements:

Table 2. Fraction of the surface area spalled after 150 and 300 cycles at 850 °C in air (sample thickness: 0.15 mm).

		Fe-18Cr	Fe-18Cr-Ti	Fe-18Cr-Nb	Fe-18Cr-TiNb
150 cycles	Spalled fraction	0	0	0	0
	Scale thickness	0.9 µm	2.8 µm	1.4 µm	1.5 µm
300 cycles	Spalled fraction	0.1%	0	0.5%	0
	Scale thickness	1.3 µm	4.0 µm	2.0 µm	2.1 µm

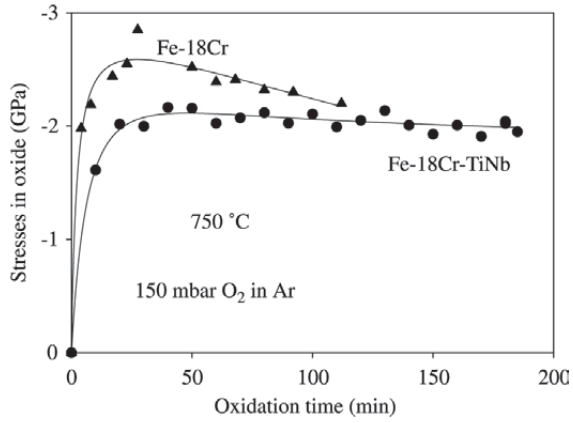

Figure 3. Oxide growth stresses at 750 °C measured by in situ Raman spectroscopy during oxidation in oxygen of the reference and bi-stabilised stainless steel grades.

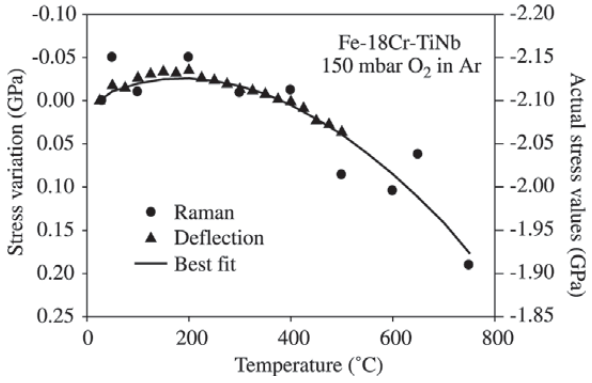

Figure 4. Stress evolution in oxide scales on Fe-18Cr-TiNb during cooling to room temperature.

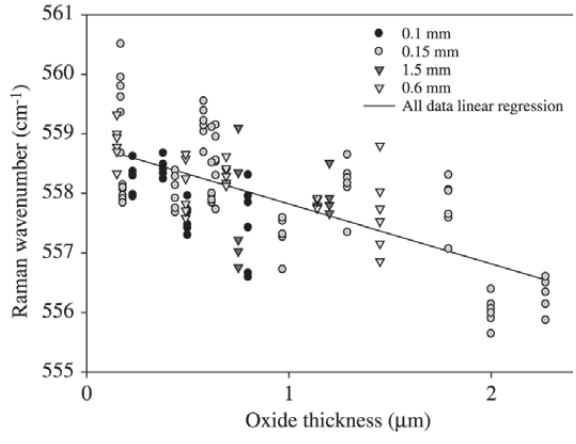

Figure 5. Room temperature Raman wavenumber as a function of oxide thickness for oxides isothermally grown on Fe-18Cr-TiNb specimens of different thickness.

- Thermal stresses were purely elastic in this domain, as the Raman shift was exactly reversible at reheating to 750 °C,
- The compressive stress value added at cooling was fairly low, near 200 MPa,
- A stress maximum seemed to be present near 200 °C, showing a tensile-compressive change of the thermal stresses at this temperature.

These conclusions were checked and more precisely quantified by continuous recording, under Ar-H_2 inert atmosphere, of the deflection of 150 μm thick samples covered by 1.5 μm thick oxide on one side only. In the 25-500 °C temperature range, deflection was exactly reversible for heating and cooling and showed excellent agreement with the Raman values, as seen from the triangle points in Fig. 4. In particular, the stress maximum was confirmed by a positive-negative change in the deflection and precisely determined to occur at 170 °C.

Residual stresses

Residual stresses, measured on the bi-stabilised grade after cooling isothermally grown oxides, showed a general tendency to be lower for higher scale thickness (Fig. 5). However, they seemed to be independent on the steel sample thickness, contrary to what was expected from the observation that spallation was greatly influenced by sample thickness.

The difference in residual stresses of scales grown at 900 °C in oxygen or in water vapour on the Fe-18Cr reference grade is presented in Fig. 6. It is observed that oxide residual stresses are higher when grown in H_2O, contrary to what is expected from the fact that no spallation was de-

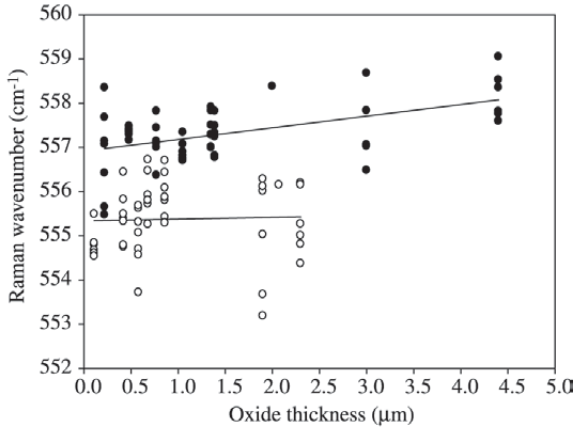

Figure 6. Evolution of the room temperature Raman wavenumber as a function of oxide scale thickness for oxides grown at 900 °C in O_2 (open circles) or H_2O (black circles) on the reference grade Fe-18Cr.

Table 3. Adhesion energy of oxide scales grown for 150 cycles and comparison with isothermally grown oxides.

Stainless steel grade	Fe-18Cr	Fe-18Cr-Ti	Fe-18Cr-Nb	Fe-18Cr-TiNb
Oxide thickness at 150 cycles (μm)	0.9	2.8	1.4	1.5
Adhesion energy ($J.m^{-2}$)	11 (± 6)	37 (± 5)	13 (± 8)	39 (± 4)
Average adhesion energy for the same thickness in isothermal conditions (from Fig. 7)	~ 140	~ 22	~ 0	~ 15

tected for such scales. The same measurements were performed on the bi-stabilised grade where the same trend was noticed.

3.3. Adhesion results

The adhesion energy of the scales formed on the 4 grades under study was measured after isothermal exposition in oxygen or water vapour for different scale thicknesses. For scales grown in cyclic conditions, the adhesion energy was determined after 150 thermal cycles. Figure 7 shows adhesion results obtained for scales isothermally grown in oxygen, where it is observed that a general trend is the decrease of the adhesion energy with scale thickness increase. The reference grade Fe-18Cr and the bi-stabilized grade Fe-18Cr-TiNb present approximately the same oxide-metal adhesion values, whereas scales on the Nb-grade seem to be less adherent, conversely more adherent on the Ti-grade.

The same measurements were performed on samples cyclically oxidised at 850 °C. The results are given in Table 3. Comparison with adhesion isothermal results in Fig. 7 shows that oxides formed in cyclic conditions were mostly more adherent, except for the reference grade which exhibited a surprising very small adhesion energy with regard to the very thin oxide scales formed.

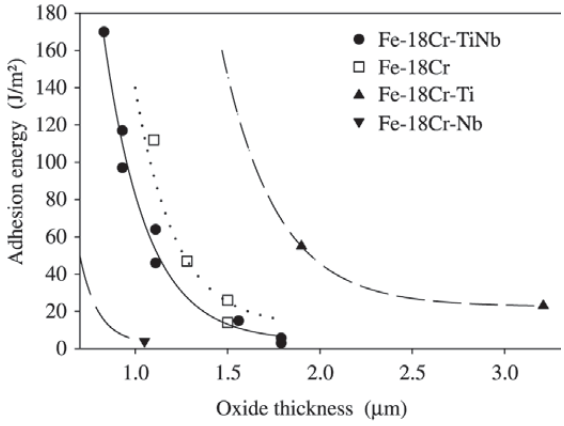

Figure 7. Isothermal oxidation at 900 °C in oxygen: adhesion energy as a function of scale thickness.

4. Discussion

Comparing spallation results for the different grades, it is concluded that it is not the thickest oxides which spall at cooling, but that a strong chemical effect of the addition element plays a major role. In particular, the Ti-grade oxidises significantly more rapidly than the others, leading to a thicker scale, but exhibits the lowest spallation. On the contrary, Nb addition, which only slightly increases the isothermal oxidation kinetics in these conditions, is highly detrimental in terms of spallation.

The oxide growth stresses determined at 750 °C lie in the GPa range as observed for chromia on Ni-Cr alloys[12,13], alumina on FeCrAl's[14,15]. Contrary to what is generally admitted, the growth stress state of the oxide scale does not seem to be a pertinent parameter to discuss spallation. For example, growth stresses were measured to be identical on the reference and on the TiNb-containing grade although the spallation difference of these materials was very different.

Thermal stresses, which are mostly evoked as the main driving force for spallation were observed in the present study to be fairly low. When discussed in the literature, they are mostly calculated from the expansion coefficient mismatch and use values of the thermal expansion coefficient of chromia generally taken from bulk determinations, ranging from 5.7 to 9.5×10^{-6} [16,17,18]. Using such values, thermal stresses are probably overestimated. The results from the present work can be used for *in situ* determination of the actual value of the Cr_2O_3 thin scale thermal expansion coefficient, as both Raman and deflection experiments have shown that oxide and metal exhibit the same value at a temperature of 170 °C (Fig. 4). Using the carefully measured steel expansion coefficient α_M variation with temperature[19]:

$$\alpha_M = 9.3 \times 10^{-6} + 3.3 \times 10^{-9} T$$

a value of 10.8×10^{-6} could be derived for α_{Cr2O3} at this temperature. This value is significantly higher than all values reported before and recalled above. Such a high value is the reason of the rather low thermal stresses determined in the present study. It must be observed that the deflection method, needing no calibration, is a very useful tool for checking the Raman results for which the biaxial-hydrostatic calibration question is a problem.

Contrary to oxide stresses, adhesion energy is a more pertinent parameter for discussing spallation, as the present

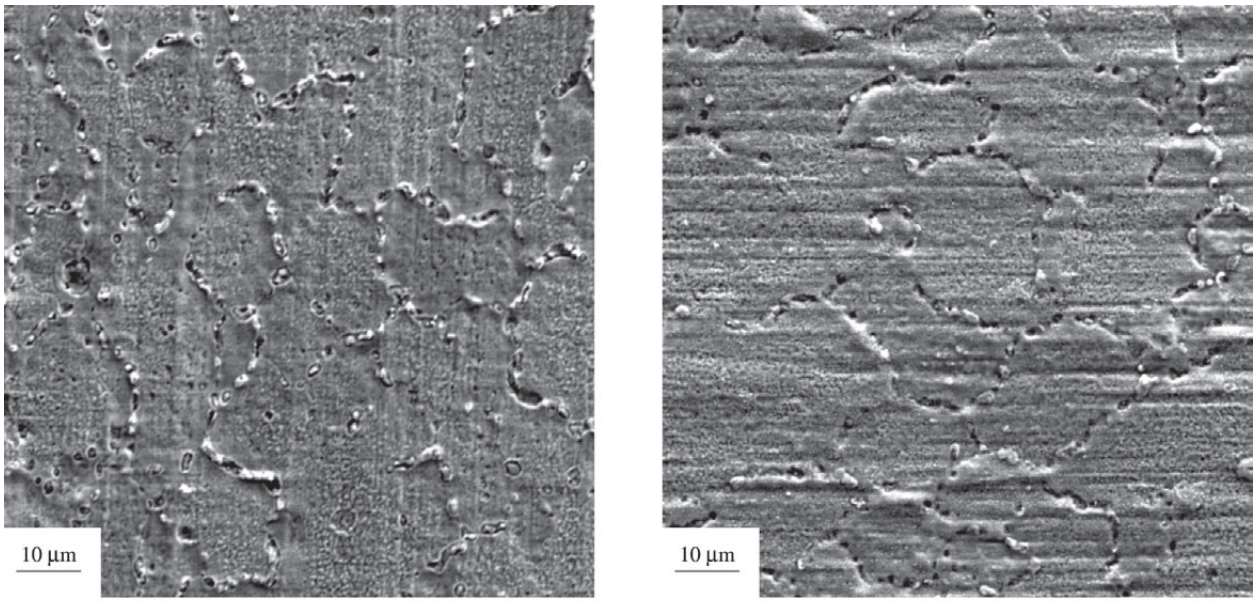

Figure 8. Metal side (left) and oxide side (right) of the Cr_2O_3/Fe-18Cr-Ti debonded interface showing TiO_2 precipitates pinned in the steel substrate (after 150 cycles at 850 °C).

measurements have shown that this parameter well describes the differences in spallation behaviour of the stainless steel grades studied. Either in isothermal or cyclic oxidation conditions, it appears that oxide-metal adhesion energy is greatly increased by the addition of titanium to 18%Cr ferritic stainless steels. Microscopic observation of cross-sections or of both sides of the steel-oxide interface after decohesion by the blister test showed that such a good behaviour was linked with titanium internal oxidation generating TiO_2 protrusions well pinned in the steel substrate (Fig. 8).

During the blister test experiments, TiO_2 protrusions were forced to break and separate from the oxide to allow scale-substrate separation. It is thought to be the same to initiate scale spallation. On the contrary, niobium addition to steel reduced the interfacial adhesion energy. In the steels, niobium was always observed as (Fe,Nb) intermetallic precipitates which were shown to act as preferential metal-oxide decohesion sites. These precipitates contain only traces of chromium and the chromia scale in contact with them was generated by lateral diffusion, presenting no parental relation, therefore bad adhesion. It is interesting to note that the bi-stabilized grade Fe-18Cr-TiNb does not differ much from the reference grade in terms of adhesion energy, probably resulting from the competitive opposite effects of Ti and Nb. However, when observing their spallation behaviour, these grades differ notably (Fig. 1), showing that other effects must be taken into account. This fact is confirmed by the comparative measurements of interfacial adhesion energy of scales grown on the same steel in oxygen or in water vapour. Comparing at the same scale thickness, the adhesion energy was shown to be only slightly higher for scales grown in H_2O, whereas the difference in spallation behaviour was much more significant (Fig. 9).

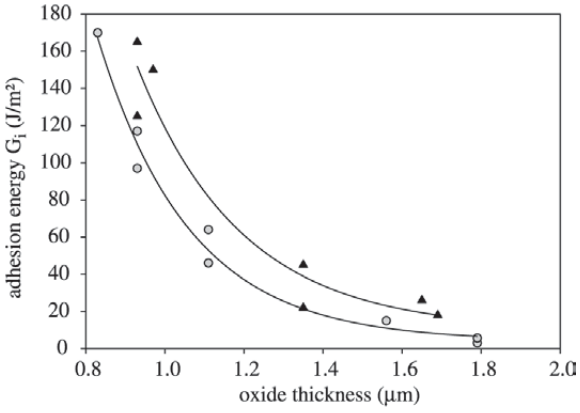

Figure 9. Adhesion energy as a function of scale thickness for oxides isothermally grown at 900 °C on Fe-18Cr-TiNb in oxygen (circles) or in water vapour (triangles). Oxidant (O_2 or H_2O) partial pressure: 150 mbar.

Observing the metal-oxide interface, either on fractures (Fig. 10) or on the pieces separated by the blister test (Fig. 11), it appears that all grades present flatter and smoother inter-

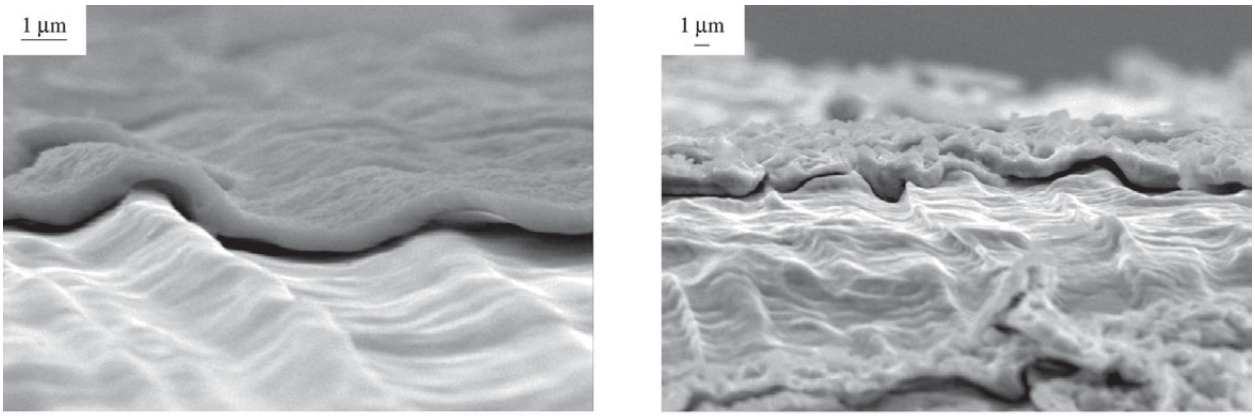

Figure 10. Surface of the Fe-18Cr steel grade observed after removing the oxide scale by bending samples oxidised at 900 °C (left : in water vapour, right: in oxygen).

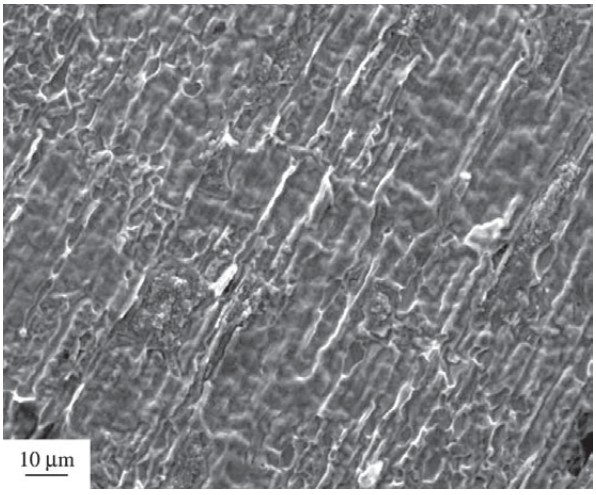

Figure 11. Metal side of the Fe-18Cr-oxide interface after scale separation by the blister test showing pronounced undulation. Oxidation in oxygen at 900 °C, oxide thickness : 1.3 µm.

faces when oxidised in water vapour, more convoluted and undulated when oxidised in oxygen. Such a ratcheting phenomenon is the result of stress relaxation, increasing the interface area and leading to a decrease in the total energy[20].

It was also observed pronounced interface undulation on thick steel samples exhibiting high spallation (Fig. 2), whereas thinner samples kept a flat interface, regularly following the ridges induced by the polishing sequence, and presenting no spallation. However these samples were shown to elongate during oxidation, showing that a competitive relaxation mode takes place according to the mechanical properties of the metallic substrate. When sample elongation cannot take place due to any geometrical or mechanical reason, interface undulation becomes the most energetic way to relax stresses, leading to local normal stress component generation during cooling and easy spallation.

5. Conclusions

Several conclusions arise from the results of the present work:

- Spallation of oxide scales grown on ferritic stainless steels depends on many parameters, among which are oxide thickness and steel minor additions, but also metal thickness and nature of the oxidising atmosphere (O_2 or H_2O);
- Growth stresses resulting from volume expansion are compressive and high soon after the onset of oxidation, reaching the 2 GPa range and stabilising during the course of the oxide growth;
- Such high stresses do not induce oxide spallation during isothermal exposure for the oxide thickness observed (≤ 2 µm);
- Spallation occurs at cooling, although the extra compressive stresses induced by the thermal mismatch are of minor value, due to the high expansion coefficient of the chromia formed, near to the rather low value for the ferritic material (this shows the necessity of determining the thermoelastic properties of real oxide scales and not using data for bulk oxides);
- High residual stresses can be observed on non-spalled oxides whereas adherent parts of highly spalled scales may exhibit lower stress;
- Adhesion energy of the metal-oxide interface, quantitatively determined using the “inverted blister test”, is

a pertinent parameter to assess the spallation behaviour of different steel grades. The respective good and bad influence of titanium and niobium in steels in terms of spallation was exactly reflected by the adhesion energies of their oxide scales;

- The reinforcement of scale adhesion by Ti addition was shown to be the result of oxide pinning by TiO_2 internal precipitates. The presence in the steels of intermetallic (Fe,Nb) precipitates was detrimental to that pinning;
- Relaxation phenomena taking place in the steel substrate seem to govern the spallation behaviour. In particular, interface undulation was shown to reduce the resistance of stainless steels to spallation, whereas sample elongation, when possible, kept a flat steel-oxide interface and spalled less;
- The observation that oxidation in water vapour led to low spallation in relation with flat steel-oxide interface is not yet understood. Effects of hydrogen on the mechanical properties of the interface must be searched;

Acknowledgments

This work described in this paper takes place in the "Oxidation" project of the GEDAI (Groupe d'Etudes sur la Durabilité des Alliages Inoxydables) at Institut National Polytechnique de Grenoble – Ecole Nationale Supérieure d'Electrochimie et d'Electrométallurgie. The financial support of the French Ministry of Education and of Arcelor Group is greatly acknowledged. Part of this work was also discussed in the Groupes de Recherches (GDR) – CNRS "Corrosion et Adhésion des Matériaux Métalliques Oxydés".

References

1. Antoni, L.; Herbelin, J.M. *Advantages of ferritic stainless steels in cyclic high temperature conditions*, in *Cyclic Oxidation of High Temperature Materials*, (eds. M. Schütze and W. J. Quadakkers), EFC Series n. 27, IOM communications, London, p. 187-197, 1999.
2. Mougin, J.; Rosman, N.; Lucazeau, G.; Galerie, A. *In-situ Raman monitoring of chromium oxide scale growth*, J. Raman Spectroscopy, v. 32, p. 739-744, 2001.
3. Birnie, J.; Craggs, C.; Gardiner, D.J.; Graves, P.R. *Ex-situ and in-situ determination of stress distribution in chromium oxide films by Raman spectroscopy*, Corr. Sci., v. 33, n. 1, p. 1-12, 1992.
4. Mougin, J.; Le Bihan, T.; Lucazeau, G. *High-pressure study of Cr_2O_3 obtained by high-temperature oxidation by X-ray diffraction and Raman spectroscopy*, J. Phys. Chem. Solids, v. 62, p. 553-563, 2000.
5. Mougin, J. *Tenue mécanique de couches d'oxyde thermique générées sur le chrome et sur quelques aciers inoxydables ferritiques : étude des contraintes et de l'adhérence*, PhD Thesis, Institut National Polytechnique de Grenoble, in French, 2001.
6. Mougin, J.; Dupeux, M.; Galerie, A.; Antoni, L.; Huntz, A.M.; Valot, C. *submitted to Oxid. Met.*
7. Renusch, D.; Grimsditch, M.; Koshelev, I.; Veal, B.W.; Hou, P.Y. *Strain determination in thermally-grown alumina scales using fluorescence spectroscopy*, Oxid. Met., v. 48, n. 5/6, p. 471-495, 1997.
8. Lipkin, D.M.; Clarke, D.R. *Measurements of the stress in oxide scales formed by oxidation of alumina-forming alloys*, Oxid. Met., v. 45, n. 3/4, p. 267-280, 1996.
9. Fernando, M.; Kinlock, A.J.; Vallerschamp, R.E.; Van der Linde, W.B. *The use of the inverted blister test to measure the adhesion of an electrocoated paint layer adhering to a steel substrate*, Mater. Sci. Lett., v. 12, p. 875-877, 1993.
10. Dupeux, M.; Bosseboeuf, A. *Application of the blister test to adhesion energy measurements in metal-ceramic film-on-substrate systems*, in *Interfacial Science in Ceramic Joining*, (eds. A. Bellosi *et al.*), Kluwer Academic Publ., NL, p. 317-327, 1997.
11. Mougin, J.; Dupeux, M.; Galerie, A.; Antoni, L. *An inverted blister test to measure the adhesion energy of thermal oxide scales on metals or alloys*, Mater. Sci. Technol., v. 18, p. 1217-1220, 2002.
12. Calvarin, G.; Huntz, A.-M.; Hugot-Le-Goff, A.; Joiret, S.; Bernard, M.-C. *Oxide scale stress determination by Raman spectroscopy ; application to the NiCr-Cr_2O_3 system and influence of yttrium*, Scripta Mater., v. 38, n. 11, p. 1649-1658, 1998.
13. Zhu, D.; Stout, J.H.; Shores, D.A. *Determination of stress gradients in a thermally grown oxide layer using X-ray diffraction*, Mater. Sci. Forum, v. 251-254, p. 333-340, 1997.
14. Bull, S.J.; *Modeling of residual stress in oxide scales*, Oxid. Met., v. 49, n. 1/2, p. 1-17, 1998.
15. Tolpygo, V.K.; Dryden, J.R.; Clarke, D.R. *Determination of the growth stress and strain in alpha-Al_2O_3 scales during the oxidation of Fe-22Cr-4.8Al-0.3Y alloy*, Acta Mater., v. 46, 3, p. 927-937, 1998.
16. Schütze, M. *Protective oxide scales and their breakdown*, Institute of Corrosion and Wiley Series, Chichester, UK, 1997.
17. Huntz, A.M.; Schütze, M. *Stresses generated during oxidation sequences and high temperature fracture*, Mater. High Temp., v. 12, n. 2/3, p. 151-161, 1994.
18. Huntz, A.-M. *Stresses in NiO, Cr_2O_3 and Al_2O_3 oxide scales*, Mater. Sci. Eng., v. A201, p. 211-228, 1995.
19. Value determined by the steel-maker (Ugine-Savoie-Imphy, ARCELOR group).
20. He, M.Y.; Evans, A.G.; Hutchinson, J.W. *The ratcheting of compressed thermally grown thin films on ductile substrates*, Acta Mater., v. 48, p. 2593-2601, 2000.